

We are IntechOpen, the world's leading publisher of Open Access books Built by scientists, for scientists

4,500

Open access books available

118,000

International authors and editors

130M

Downloads

Our authors are among the

154

Countries delivered to

TOP 1%

most cited scientists

12.2%

Contributors from top 500 universities



WEB OF SCIENCE™

Selection of our books indexed in the Book Citation Index
in Web of Science™ Core Collection (BKCI)

Interested in publishing with us?
Contact book.department@intechopen.com

Numbers displayed above are based on latest data collected.
For more information visit www.intechopen.com



Introductory Chapter: An Introduction to the Optimization of Composite Structures

Karam Maalawi

Additional information is available at the end of the chapter

<http://dx.doi.org/10.5772/intechopen.81165>

1. Introduction

Structural applications of composite materials are increasing in several engineering areas where high stiffness and strength-to-weight ratios, long fatigue life, superior thermal properties, and corrosive resistance are most beneficial [1–4]. Common types include laminated composites [5], functionally graded material (FGM) structures, and nanocomposites as well as smart composite structures [6]. In fact composite structures are usually tailored, depending upon the specific objectives, by choosing the individual constituent materials and their volume fractions, fiber orientation angles, and lamina thickness and number, as well as the fabrication procedure. To attain the best results, adequate optimization models have to be implemented to find practical optimal solutions satisfying a given set of design constraints.

This introductory chapter provides a brief review on the optimum design of composite structures and the relevant optimization techniques that are capable of finding the needed optimal solutions. Several problems can be addressed, including the structural design for maximum stability, maximum natural frequencies, and minimum mass or maximum stiffness subject to limits on strength, deflections, and side constraints. The relevant design variables include geometrical dimensions and material properties as well. A numerical example is given at the end of this chapter to demonstrate a real and practical application of the optimum composite structures.

2. The optimal design problem

Several research papers and text books exist in the field of optimal design of composite structures with a variety of valuable applications in civil, mechanical, ocean, and aerospace engineering. An important stage has now been reached at which an investigation of such

developments and their practical possibilities should be made and presented. Two distinct review papers have been published covering the development of the optimum design of composites over more than 40 years. The first paper by Sonmez [7] presented a comprehensive survey for more than 1000 journal papers, conference papers, textbooks, and web links from the year 1969 to 2009. Sonmez classified the papers according to the type of the composite structure, loading conditions, optimization model, failure criteria, and the utilized search algorithm. The second paper by Ganguli [8] covered a historical review from 1973 to 2013. It provides the growth of the field by including more than 90 references dealing with a variety of optimization methods utilized for tailoring composites to achieve certain design objectives. Applications of several optimization techniques were presented, including feasible direction methods, sequential quadratic programming, and stochastic optimization such as particle swarm and ant colony algorithms. Ganguli classified the published work into five categories named pioneering research for the work published in the 1970s, early research in the 1980s, moving toward design in the 1990s, the new century in the 2010s, and the current research for papers published after 2010.

In general, design optimization seeks the best values of **design variables**, $\underline{X}_{n \times 1}$, to achieve, within certain **constraints**, $\underline{G}_{m \times 1}(\underline{X})$ placed on the system behavior, allowable stresses, geometry, or other factors; its goal of optimality is defined by the a vector of **objective functions**, $\underline{F}_{k \times 1}(\underline{X})$, for specified environmental conditions. Mathematically, design optimization may be cast in the following standard form [9]:

Find the set of design variables $\underline{X}_{n \times 1}$ that will

$$\text{minimize } F(\underline{X}) = \sum_{i=1}^k w_{f_i} F_i(\underline{X}) \quad (1)$$

$$\text{subject to } G_j(\underline{X}) \leq 0, j = 1, 2, \dots, I \quad (2)$$

$$G_j(\underline{X}) = 0, j = I + 1, I + 2, \dots, m \quad (3)$$

where w_{f_i} is the weighting factors measuring the relative importance of $F_i(\underline{x})$ with respect to the overall design goal:

$$\begin{aligned} 0 &\leq w_{f_i} \leq 1 \\ \sum_{i=1}^k w_{f_i} &= 1 \end{aligned} \quad (4)$$

Figure 1 shows the overall structure of an optimization approach to design. Major objectives in mechanical and structural engineering involve minimum fabrication cost, maximum product reliability, maximum stiffness/weight ratio, minimum aerodynamic drag, maximum natural frequencies, maximum critical shaft speeds, etc. Design variables describe configuration, dimensions and sizes of elements, and material properties as well. In the design of structural components, such as those of an automobile structure, the main design variables represent the thickness of the covering skin panels and the spacing, size, and shape of the transverse and

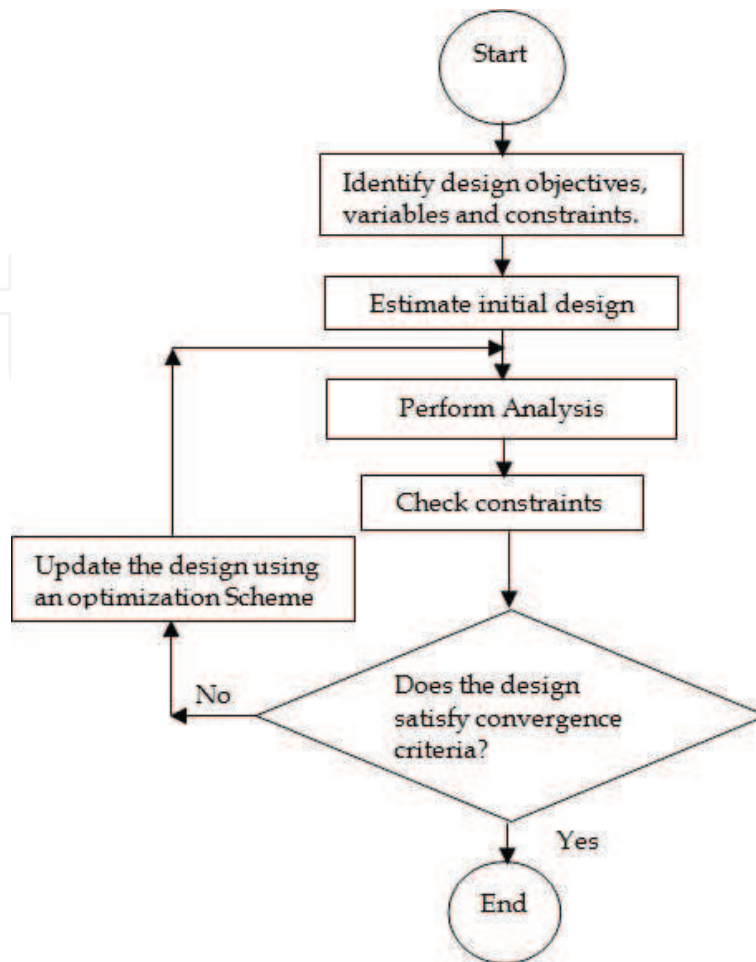


Figure 1. Design optimization process.

longitudinal stiffeners. The sizes of the constituent elements of the system are measured by such properties as the cross-sectional dimensions, section areas, area moments of inertia, torsional constants, plate's thicknesses, etc. If the skin and/or stiffeners are made of layered composites, the orientation of the fibers and their proportion can become additional variables. If one optimizes for configuration, the design variables will include spatial coordinates. Also, in dynamic problems, the location of nonstructural masses and their magnitudes can be additional design variables.

3. Optimization techniques

The class of optimization problems described by Eqs. (1)–(3) may be thought of as a search in an n -dimensional space for a point corresponding to the minimum value of the overall objective function and such that it lies within the region bounded by the subspaces representing the constraint functions. Iterative techniques are usually used for solving such optimization problems in which a series of directed design changes (moves) are made between successive points in the design space. Several optimization techniques are classified according to the way of

selecting the search direction [9]. The most commonly used approaches are the random search, conjugate directions, and conjugate gradients methods. Other algorithms for solving global optimization problems may be classified into heuristic methods that find the global optimum only with high probability and methods that guarantee to find a global optimum with some accuracy. The simulated annealing technique and the genetic algorithms (GAs) belong to the former type, where analogies to physics and biology to approach the global optimum are utilized. The simulated annealing technique is an iterative search method based on the simulation of thermal annealing of critically heated solids. Hasancebi et al. [10] applied it to find the optimum design of fiber composite structures as an efficient method to solve multi-objective optimization models. On the other hand, the GAs [11, 12] are based on the principles of natural genetics and natural selection. GAs do not utilize any gradient information during the searching process. Narayana Naik et al. [12] used GA and various failure mechanisms based on different failure criteria to reach an optimal composite structure. Another robust algorithm in solving complex problems of optimal structural design is named particle swarm optimization algorithm (PSOA). This algorithm is based on the behavior of a colony of living things, such as a swarm of insects like ants, bees, and wasps, a flock of birds, or a school of fish. Omkar et al. [13] applied PSOA to achieve a specified strength with minimizing weight and total cost of a composite structure under different failure criteria. To the author's knowledge, GA has been the most efficient stochastic method for obtaining the global optimum design of composite structures.

4. Application: buckling optimization of anisotropic cylindrical shells

Structural buckling failure due to high external hydrostatic pressure is a major consideration in designing cylindrical shell-type structures. This section presents a direct approach for enhancing buckling stability limits of thin-walled long cylinders that are fabricated from multi-angle fibrous laminated composite lay-ups. The mathematical formulation employs the classical lamination theory for calculating the critical buckling pressure, where an analytical solution that accounts for the effective axial and flexural stiffness separately as well as the inclusion of the coupling stiffness terms is presented. The associated design optimization problem of maximizing the critical buckling pressure has been formulated in a standard nonlinear mathematical programming problem with the design variables encompassing the fiber orientation angles and the ply thicknesses as well. The physical and mechanical properties of the composite material are taken as preassigned parameters. The proposed model deals with dimensionless quantities in order to be valid for thin shells having different thickness-to-radius ratios. Results have been obtained for cases of filament wound cylinders fabricated from different types of composite materials.

The basic analysis and analytical formulation presented in this chapter are based on the work given by Maalawi [14], which provides good sensitivity to lamination parameters and allows the search for the needed optimal stacking sequences in a reasonable computational time. Referring to the structural model depicted in **Figure 2**, the significant strain components are

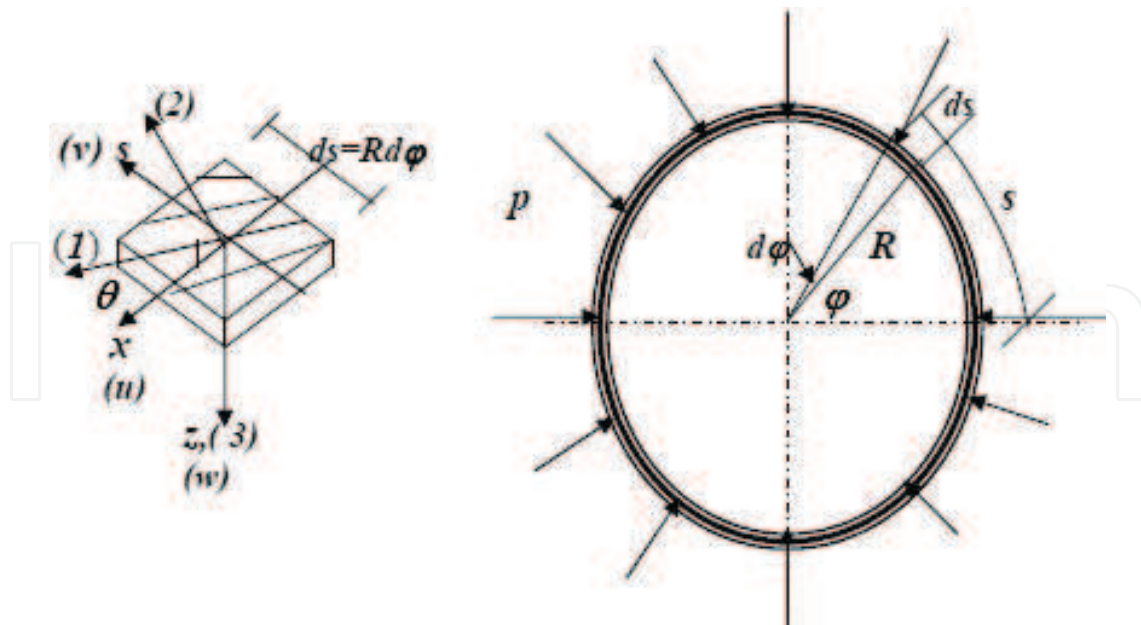


Figure 2. Laminated composite cylindrical shell under external pressure (u displacement in the axial direction x , v in the tangential direction s , w in the radial direction z).

the hoop strain (ϵ_{ss}^0) and the circumferential curvature (κ_{ss}) of the mid-surface. The reduced form of the stress-strain relationships in matrix form is

$$\begin{Bmatrix} N_{ss} \\ M_{ss} \end{Bmatrix} = \begin{bmatrix} A_{22} & B_{22} \\ B_{22} & D_{22} \end{bmatrix} \begin{Bmatrix} \epsilon_{ss}^0 \\ \kappa_{ss} \end{Bmatrix} \quad (5)$$

where N_{ss} and M_{ss} are the resultant distributed force and moment and (A_{ij} , B_{ij} , D_{ij}) are the extensional, coupling, and bending stiffness coefficients, respectively [1].

4.1. Analytical buckling model

The governing differential equations of anisotropic long cylinders subjected to external pressure are cast in the following:

$$M'_{ss} + R(N'_{ss} - \beta N_{ss}) = \beta p R^2 \quad (6.1)$$

$$M''_{ss} - R[N_{ss} + (\beta N_{ss})' + p(w_o + v'_o)] = p R^2 \quad (6.2)$$

where u_o , v_o , and w_o are the displacements of a generic point (x, s) on the shell middle surface ($z = 0$) in x , s , and z directions, respectively. The prime denotes differentiation with respect to the angular position ϕ and $\beta = (v_o - w'_o)/R$. For the case of thin cylinders with thickness-to-radius ratio $(h/R) \leq 0.1$, the critical buckling pressure can be determined using the mathematical expression [14]:

$$p_{cr} = 3 \left[\frac{D_{22}}{R^3} \right] \left[\frac{1 - (\psi^2/\alpha)}{1 + \alpha + 2\psi} \right] \quad (7.1)$$

$$\psi = \left(\frac{1}{R} \right) \left(\frac{B_{22}}{A_{22}} \right) \quad (7.2)$$

$$\alpha = \left(\frac{1}{R^2} \right) \left(\frac{D_{22}}{A_{22}} \right) \quad (7.3)$$

4.2. Definition of the baseline design

It is convenient first to normalize all variables and parameters with respect to a baseline design, which has been selected to be a unidirectional orthotropic laminated cylinder with the fibers parallel to the shell axis x . Optimized designs shall have the same material properties, mean radius R , and total shell thickness h of the baseline design. Expressions for calculating the critical buckling pressure (P_{cro}) of the baseline design are defined in **Table 1**, which depend upon the type of composite material utilized and the shell thickness-to-radius ratio (h/R) as well.

4.3. Optimization model

The search for the optimized lamination can be performed by coupling the analytical buckling shell model to a standard nonlinear mathematical programming procedure. The resulting optimization problem may be cast in the following standard form to

$$\text{minimize} \quad -\hat{p}_{cr} \quad (8.1)$$

$$\text{subject to} \quad h_L \leq \hat{h}_k \leq h_U, \quad (8.2)$$

$$\theta_L \leq \theta_k \leq \theta_U \quad k = 1, 2, \dots, n \quad (8.3)$$

$$\sum_{k=1}^n \hat{h}_k = 1 \quad (8.4)$$

where $\hat{p}_{cr} = p_{cr}/p_{cro}$ is the dimensionless critical buckling pressure, and (h_L, h_U) are the lower and upper bounds imposed on the individual dimensionless ply thicknesses $\hat{h}_k = h_k/h$.

Material type	Orthotropic mechanical properties* (GPa)				$P_{cro} \times (h/R)^3$ (GPa)
	E_{11}	E_{22}	G_{12}	ν_{12}	
E-Glass/vinyl ester	41.06	6.73	2.5	0.299	1.708
Graphite/epoxy	130.0	7.0	6.0	0.28	1.757
S-Glass/epoxy	57.0	14.0	5.7	0.277	3.567

* E_{11} = longitudinal modulus, E_{22} = hoop modulus, ν_{12} = Poisson's ratio for axial load, $\nu_{21} = \nu_{12}E_{22}/E_{11}$.

Table 1. Material properties and critical buckling pressure of the baseline design (P_{cro}).

According to the filament-winding manufacturing process, each ply is characterized by its angle θ_k with respect to the cylinder axis x . The stacking sequence is denoted by $[\theta_1/\theta_2/\dots/\theta_n]$, where the angles are given in degrees, starting from the outer surface of the shell. In addition, in a real-world manufacturing process, the filament-winding angles θ_k must be chosen from a limited range of allowable lower (θ_L) and upper (θ_U) values according to technology references. It is important to mention here that the volume fractions of the constituent materials of the composite structure is assumed to not significantly change during optimization, so that the total structural mass remains constant at its reference value of the baseline design.

4.4. Optimal solutions

The functional behavior of the candidate objective function, as represented by maximization of the dimensionless buckling pressure \hat{p}_{cr} , is thoroughly investigated in order to see how it is changed with the optimization variables in the selected design space. The final optimum designs recommended by the model will directly depend on the mathematical form and behavior of the objective function.

4.4.1. Two-layer anisotropic long cylinder

The first case study to be considered herein is a long thin-walled cylindrical shell fabricated from E-glass/vinyl ester composites with the lay-up composed of only two plies ($n = 2$) having equal thicknesses ($\hat{h}_1 = \hat{h}_2 = 0.5$) and different fiber orientation angles. Considering the case of $\pm 63^\circ$ angle ply, the present model gives $\hat{p}_{cr} = 4.23$, i.e., $P_{cr} = 4.23 \times 1.708 \times (h/R)^3$ GPa, depending on the shell thickness-to-radius ratio. The actual dimensional values of the critical buckling pressure for the different thickness ratios are given in **Table 2** for the cases of baseline design $[0^\circ]$, helically wound $[\pm 63^\circ]$, and $[\pm 90^\circ]$ hoop layers. The unconstrained maximum value of $\hat{p}_{cr} = 6.1$ occurs at the design points $[\theta_1/\theta_2] = [\pm 90, \pm 90]$.

For a two-ply long cylinder fabricated from graphite/epoxy composites, **Figure 3** shows the developed level curves of the dimensionless buckling pressure, \hat{p}_{cr} (also named isomerits or isobars) in the $(\theta_1 - \theta_2)$ design space. As seen in the figure, the maximum value of \hat{p}_{cr} reaches a value of 18.57 for a hoop wound construction. **Table 3** presents the solutions for the $[\pm 45^\circ]$ angle-ply and the $[90^\circ]$ cross-ply constructions for different thickness-to-radius ratios. These solutions

	Baseline $[0^\circ]$	Helically wound $[\pm 63^\circ]$	Hoop plies $[\pm 90^\circ]$
	$\hat{p}_{cr} = 1.00$	4.23	6.10
(h/R)			
(1/15)	506.07	2140.69	3087.05
(1/20)	213.50	903.11	1302.35
(1/25)	109.31	462.39	666.80
(1/50)	13.66	57.80	83.35

$[P_{cr} = \hat{p}_{cr} \times 1.708 \times 10^6 (h/R)^3 \text{ KPa}]$.

Table 2. Critical buckling pressure for E-glass/vinyl ester cylinder with different lay-ups.

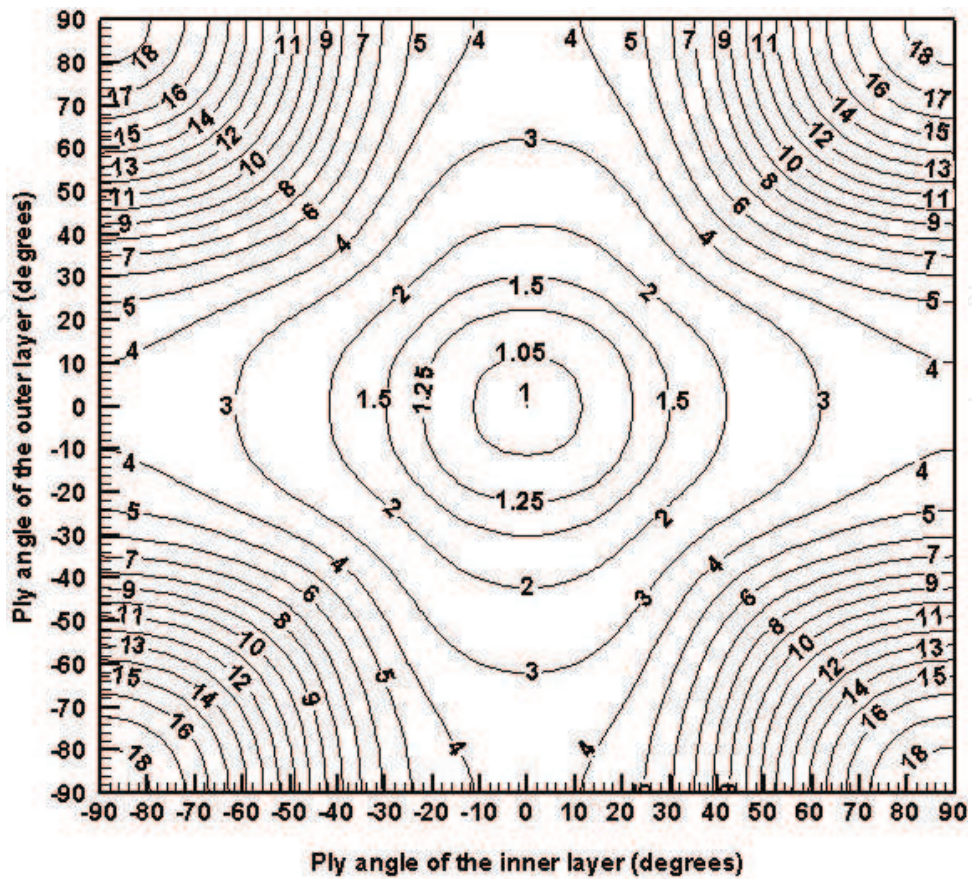


Figure 3. \hat{p}_{cr} -isomerits for a graphite/epoxy, two-layer cylinder in $[\theta_1/\theta_2]$ design space ($\hat{h}_1 = \hat{h}_2 = 0.5$).

are also valid for lay-ups $[0_3]_s$, $[90_3]_s$, $[45_2/-45_2]_s$, and $[45/-45/45/-45]_s$. The case of a helically wound lay-up construction $[+\theta/-\theta]$ with unequal ply thicknesses \hat{h}_1 and \hat{h}_2 , such that their sum is held fixed at a value of unity, has also been investigated. Computer solutions have shown that no significant change in the resulting values of the critical buckling pressure can be remarked in spite of the wide change in the ply thicknesses. This is a natural expected result since the stiffness coefficients A_{22} , B_{22} , and D_{22} remain unchanged for such lay-up construction.

	Baseline $[0^\circ]$	Helically wound $[\pm 45^\circ]$	Hoop plies $[\pm 90^\circ]$
	$\hat{p}_{cr} = 1.00$	5.9	18.57
(h/R)			
(1/15)	520.59	3071.50	9667.40
(1/50)	14.06	82.93	261.02
(1/120)	1.02	5.99	18.88

$$[P_{cr} = \hat{p}_{cr} \times 1.757 \times 10^6 (h/R)^3 \text{ KPa}].$$

Table 3. Critical buckling pressure, P_{cr} for graphite/epoxy cylinder with different lay-ups.

	Baseline [0°_3]	$[0^\circ/90^\circ/0^\circ]$	$[90^\circ/0^\circ/90^\circ]$
	$\hat{p}_{cr} = 1.00$	1.651	17.92
<i>(h/R)</i>			
(1/15)	520.59	859.57	9331.19
(1/50)	14.06	23.21	251.94
(1/120)	1.02	1.68	18.23
$[P_{cr} = \hat{p}_{cr} \times 1.757 \times 10^6 (h/R)^3 \text{ KPa}]$.			

Table 4. Critical buckling pressure, P_{cr} for graphite/epoxy cylinder $[\theta_1/\theta_2/\theta_1]$.

4.4.2. Three-layer anisotropic long cylinder

Results for a cylinder constructed from three, equal-thickness layers with stacking sequence denoted by $[\theta_1/\theta_2/\theta_1]$ are given in **Table 4**. The same behavior can be observed as before but with slight change in the attained values. It was found that for the range $-30^\circ > \theta_1 > 30^\circ$ the critical buckling pressure is not much affected by variation in the ply angle θ_2 . A substantial increase in the critical buckling pressure by changing the ply angles can be observed. Similar solutions were obtained for the stacking sequences $[0^\circ_2/90^\circ]_s$ and $[90^\circ_2/0^\circ]_s$.

4.4.3. Four-layer sandwiched anisotropic cylinder

The same graphite/epoxy cylinder is reconsidered here with changing the stacking sequence to become $\pm 20^\circ$ equal-thickness layers sandwiched in between outer and inner 90° hoop layers with unequal thicknesses, i.e., $(\hat{h}_2 = \hat{h}_3)$ and $(\hat{h}_1 \neq \hat{h}_4)$, such that the thickness equality constraint $\sum_{k=1}^4 \hat{h}_k = 1$ is always satisfied. **Figure 4** shows the developed \hat{p}_{cr} -isomerits in the (\hat{h}_1, \hat{h}_2) design space. The contours inside the feasible domain, which is bounded by the three lines $\hat{h}_1 = 0$ and $\hat{h}_2 = 0$ and $\hat{h}_1 + 2\hat{h}_2 = 1$ (i.e., $\hat{h}_4 = 0$), are obliged to turn sharply to be asymptotes to the line $\hat{h}_4 = 0$, in order not to violate the thickness equality constraint. This is why they appear in the figure as zigzagged lines. At the design point $(\hat{h}_1, \hat{h}_2) = (0.25, 0.25)$, the dimensionless buckling pressure $\hat{p}_{cr} = 16.43$ (see **Figure 4** and **Table 5**). As a general observation, as the thickness of the hoop layers increases, a substantial increase in the critical buckling pressure will be achieved, e.g., at $(\hat{h}_1, \hat{h}_2) = (0.33, 0.17)$, $\hat{p}_{cr} = 17.92$ representing a percentage increase of $(17.92 - 16.43)/16.43 = 9.1\%$.

Finally, the obtained results have indicated that the optimized laminations induce significant increases, always exceeding several tens of percent, of the buckling pressures with respect to the reference or baseline design. It is assumed that the volume fractions of the composite material constituents do not significantly change during optimization, so that the total structural mass remains constant. It has been shown that the overall stability level of the laminated composite shell structures under considerations can be substantially improved by finding the optimal stacking sequence without violating any imposed side constraints. The stability limits

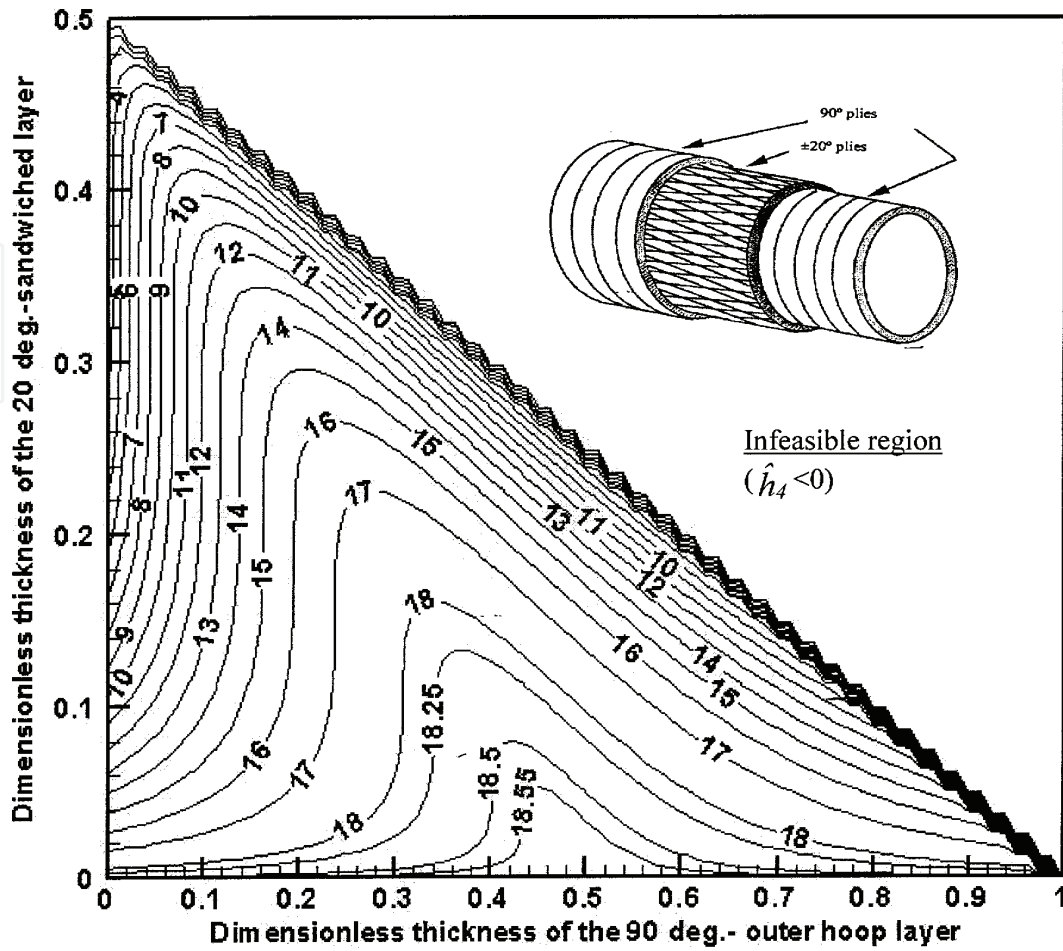


Figure 4. Design space for a sandwich lay-up graphite/epoxy cylinder [90/±20/90].

(h/R)	(1/15)	(1/20)	(1/25)	(1/50)
P_{cr}	8553.0	3609.3	1847.5	231.0

$[\hat{p}_{cr} = 16.43, P_{cro} = 1.757 \times 10^6 (h/R)^3 \text{ KPa}, P_{cr} = \hat{p}_{cr} \times P_{cro}]$.

Table 5. Critical buckling pressure, P_{cr} (KPa), for graphite/epoxy cylinder [90/±20/90].

of the optimized shells have been substantially enhanced as compared with those of the reference or baseline designs.

Author details

Karam Maalawi

Address all correspondence to: maalawi@netscape.net

National Research Centre, Cairo, Egypt

References

- [1] Daniel I, Ishai O. Engineering Mechanics of Composite Materials. 2nd ed. Oxford University Press, New York; 2006. 432p. ISBN: 978-0195150971
- [2] Kollar LP, Springer GS. Mechanics of Composite Structures. 1st ed. United Kingdom: Cambridge University Press; 2009. 500p. ISBN: 978-0521126908
- [3] Niu MCY. Composite Airframe Structures. 3rd ed. Hong Kong: Hong Kong Conmilit Press Ltd; 2011. 500p. ISBN: 978-9627128069
- [4] Kassapoglou C. Design and Analysis of Composite Structures: With Applications to Aerospace Structures. 2nd ed. New Jersey: Wiley; 2013. 410p. ISBN: 978-1118401606
- [5] Ye J. Laminated Composite Plates and Shells, 3D Modelling. 1st ed. London: Springer-Verlag; 2003. DOI: 10.1007/978-1447100959. 273p. ISBN: 978-1447100959
- [6] Kumar SS. Smart Composite Structures. 1st ed. United States: Lambert Academic Publishing; 2013. 180p. ISBN: 978-3659322532
- [7] Sonmez FO. Optimum design of composite structures: A literature survey (1969–2009). Journal of Reinforced Plastics and Composites. 2017;**36**(1):3-39. DOI: 10.1177/0731684416668262
- [8] Ganguli R. Optimal design of composite structures: A historical review. Journal of the Indian Institute of Science. 2013;**93**(4):557-570. ISSN: 0970-4140 Coden-JIISAD
- [9] Maalawi K, Badr M. Design optimization of mechanical elements and structures: A review with application. Journal of Applied Sciences Research. 2009;**5**(2):221-231
- [10] Hasancebi O, Carba S, Saka M. Improving the performance of simulated annealing in structural optimization. Structural and Multidisciplinary Optimization. 2010;**41**:189-203
- [11] Walker M, Smith RE. A technique for the multi-objective optimization of laminated composite structures using genetic algorithms and finite element analysis. Composite Structures. 2003;**62**:123-128
- [12] Narayana Naik G, Gopalakrishnan S, Ganguli R. Design optimization of composites using genetic algorithms and failure mechanism based failure criterion. Composite Structures. 2008;**83**:354-367
- [13] Omkar SN, Senthilnath J, Khandelwal R, Narayana Naik G, Gopalakrishnan S. Artificial bee colony (ABC) for multi-objective design optimization of composite structures. Applied Soft Computing. 2011;**11**(1):489-499
- [14] Maalawi KY. Optimal buckling design of anisotropic rings/long cylinders under external pressure. Journal of Mechanics of Materials and Structures. 2008;**3**(4):775-793

